EFFECT OF GRAPHENE ON THE MULTISCALE COMPOSITE PRODUCTION THROUGH ANALYTICAL PROCESS MODELLING

Mazaheri Karvandian, F[12], Hubert, P[12]*
[1] Department of Mechanical Engineering, McGill University, Montreal, Canada
[2] Research Centre for High Performance Polymer and Composite Systems (CREPEC), McGill University, Montreal, Canada
* Corresponding author (pascal.hubert@mcgill.ca)

Keywords*: Compression resin transfer moulding, multiscale composites, process modelling*

ABSTRACT

With the recent surge in the development of electric vehicles, where composites are the first choice for weight reduction, it is important more than ever to combine structural and non-structural parts into one multifunctional composite part. One of the methods to create multi-functionality and increase composites performance is through multiscale composites where a third nanoscale constituent—e.g., graphene (GP), is incorporated into a fibre-reinforced composite. Compression resin transfer moulding (C-RTM) is being used for manufacturing of composite parts in ground transportation industry since it has rapid cycles and is very cost-effective compared to vacuum-assisted processes. By adding graphene to the resin system, the thermochemical and rheological properties change and consequently, some of the processing parameters such as filling time and temperature need to be adjusted. The objective of this work is to study the impact of graphene addition to the projected production. Different contents of graphene are added to a fast-curing polyester resin system and the thermochemical and rheological properties of the GP-modified resin are evaluated. Afterwards, the total force and flow fronts are calculated using Darcy's law for representative geometries and processes. Then using analytical equations, the filling time is calculated at different part lengths. Later, this information is converted to a filling time map for different lengths and graphene contents. This will set up a cost-effective pathway for manufacturers to equip themselves for the projected changes in their production.

1 INTRODUCTION

A recent topic of interest in composites is multiscale multifunctional composites which is obtained by incorporating a nanoscale component in traditional fibre reinforced polymer composites (FRPC) [1]. Graphene is one of the nanoparticles that is of interest for this application. It was first discovered by Novoselov et al. [2] and has a honeycomb structure of single-atom-thick sheet of sp^2 hybridized carbon atoms. Due to the large specific surface area and remarkable electrical, thermal and mechanical properties, graphene is one of the top choices for incorporation in multiscale composites [3]. Studies have shown that incorporating graphene in the FRPC can increase the toughness of the brittle polymer matrix [4]. Graphene particles create a network through the polymer matrix after a certain graphene content. After this critical content, which is called percolation threshold, there is a sharp increase in the properties such as electrical conductivity [5].

Various methodologies were studied to produce graphene and to this date cost is one of the biggest issues for industrial applications, especially ground transportation. Recently, mass-produced graphene powders have become

available in the market and created an opportunity to adapt them in different composite manufacturing processes [6–8]. The method that is used in the production of these graphene particles, affects their final properties. Thus, in some cases, large loadings of graphene are required to observe a significant change in the electrical and thermal conductivity. Contrarily, at large loadings, the mechanical properties of the part could deteriorate due to re-agglomeration of particles [9, 10]. Another parameter that is subject to change with addition of graphene is the processability of the composite. Compression resin transfer moulding (C-RTM) is a composite manufacturing process which has very fast cycles and is highly cost effective compared to processes such as high-pressure resin transfer moulding (HP-RTM) and vacuum-assisted resin transfer moulding (VA-RTM) [11]. Each C-RTM processing cycle has two main stages. The first one is resin application where the resin is applied on the preform, via injection or spraying. In this stage, the mould cavity has a greater height than the final part thickness. In the second stage, after the required amount of resin is Incorporated, the top platen lowers until the final desired thickness, compressing the preform and forcing the resin to redistribute through the whole part (compaction). Lastly, the cured part is demoulded [12]. Ensuring that there are no defects in the final requires to understand the governing phenomena in the manufacturing process. Incorporating graphene in FRPCs can affect the processability of the composite as it can change the gel time, gel temperature and the viscosity of the nanomodified resin. Depending on the graphene content, the manufacturing process might be able to adapt these new parameters and some limitations of the CRTM process are identified.

In this study, the effect of different graphene contents on the gel temperature and viscosity of a nanomodified thermoset resin are investigated using a differential scanning calorimeter and rheometer. Then a set of analytical solutions are used to study the effect of viscosity changes on the processability of a glass fibre reinforced composite.

2 ANALYTICAL SOLUTIONS

There has been significant effort and progress in numerical simulation of RTM processes. Specific commercial simulation software and packages are required to solve complex equations and predict information such as mould filling times, tooling forces, residual stresses, etc [13]. Depending on the complexity of the part, these simulations may take long time to finish. Analytical solutions use simple equations considering one-dimensional flow; thus, a large number of equations can be performed in a shorter time. Although at first glance one might be sceptical of accuracy of analytical solutions, it has been proven that for simple to moderate geometries, the results are very comparable to those of numerical simulations.

The analytical equations for mould filling time and tooling forces for C-RTM processes are explained in more detail in the work of Hubert and Demaria [14] and Bickerton and Abdullah [15]. Figure 1 shows the resin flow conditions considered in the current work: in-plane radial, in-plane rectilinear and transverse rectilinear. Flow of the resin through the porous preform can be described like the flow of a Newtonian fluid through a porous medium. Thus, this flow can be modelled using the Darcy's law assuming that the resin viscosity remains constant during mould filling. Three sets of equation summarized in Tables 1-3 are developed for each flow type: injection stage and compression stage.

In Tables 1-3, t_{fill} is the time it takes for the resin to fill the mould completely, ϕ is the preform porosity. The resin viscosity if denoted by μ and is assumed to be constant during the injection and compaction stages. K is the preform permeability, σ is the compression stress and P_{inj} is the injection pressure. r_f and x_f are the distance at the flow front position and r_i is the radius of the injection port, h is the cavity height and $\dot{h}$ is the mould closing rate. F_{fluid}

is the fluid force and F_{fibre} is the force generated because of the preform compression, thus, the total clamping force is therefore the sum of F_{fluid} and F_{fibre}.

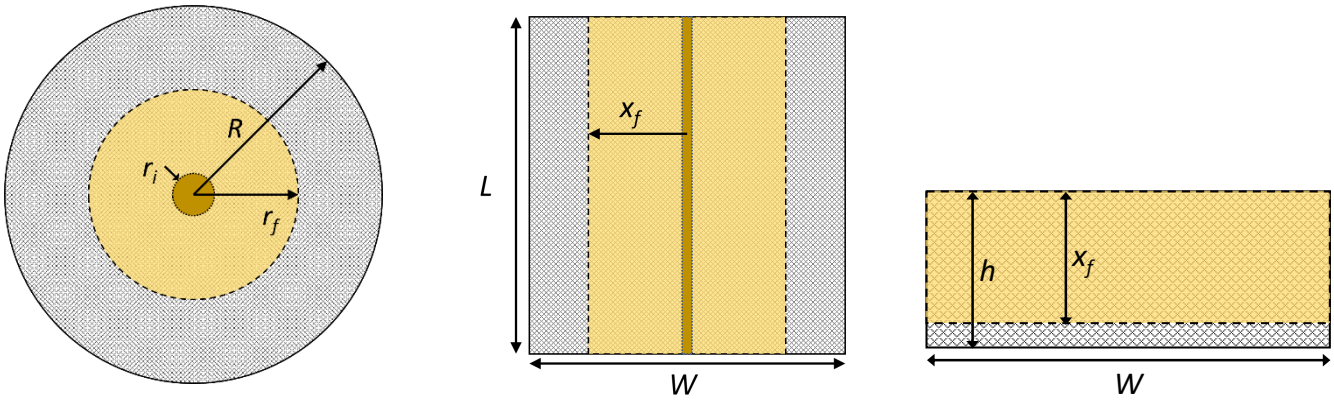

(a) (b) (c)

Figure 1. Schematic of the geometries investigated: (a) in-plane radial, (b) in-plane rectilinear, (c) transverse rectilinear. *L*, *W* and *h* are the preform length, width and thickness respectively, *R* is the preform radius, x_f or r_f is the resin flow front position.

Table1. Analytical solutions for in-plane radial flow.

Description	Injection stage	Compression stage
Filling time	$t_{fill} = \frac{\phi\mu}{2KP_{inj}}\left(r_f^2 ln\left(\frac{r_f}{r_i}\right) + \frac{r_i^2 - r_f^2}{2}\right)$	$t_{compression}$
Platen force due to the resin	$F_{fluid} = \frac{2\pi P_{inj}}{ln(r_i/r_f)}\left(\frac{r_i^2}{2} ln\left(\frac{r_f}{r_i}\right) - \frac{1}{4}(r_f^2 - r_i^2)\right)$	$F_{fluid} = \frac{\pi\mu\dot{h}}{4Kh}\left(-\frac{r_f^4}{2} + 2r_i^2 r_f^2 - \frac{3r_i^4}{2} + 2r_i^4 ln(r_i/r_f)\right)$
Platen force due to fibres compaction	$F_{fibre} = 0$	$F_{fibre} = \sigma\pi(R^2 - r_i^2)$

Table 2. Analytical solutions for in-plane rectilinear flow.

Description	Injection stage	Compression stage
Filling time	$t_{fill} = \frac{\phi\mu x_f^2}{2KP_{inj}}$	$t_{compression}$
Platen force due to the resin	$F_{fluid} = P_{inj} L x_f$	$F_{fluid} = -\frac{2\mu\dot{h}L}{3Kh} x_f^3$
Platen force due to fibres compaction	$F_{fibre} = 0$	$F_{fibre} = \sigma WL$

Table 3. Analytical solutions for transverse rectilinear flow.

Description	Injection stage	Compression stage
Filling time	$t_{fill} = \frac{WL\phi x_f}{Q_0}$	$t_{compression}$
Platen force due to the resin	$F_{fluid} = 0$	$F_{fluid} = -\frac{\dot{h}\mu WLx_f}{K}$
Platen force due to fibres compaction	$F_{fibre} = 0$	$F_{fibre} = \sigma WL$

3 EXPERIMENTAL METHODS

3.1 Materials

The resin system in this study is Polylite 31520-12, an RTM class unsaturated polyester containing calcium carbonate filler, and the curing agent used for this resin is Norox 750. The graphene used in this project is commercially available by the name GrapheneBlack 3X. All materials are provided by NanoXplore Inc.

3.2 Nanocomposite manufacturing

Overall, three batches of resin mixture were prepared with different graphene contents (0 – 7 wt% GP) as summarized in Table 4. To prepare these batches, appropriate amounts of graphene were mixed with the Polylite 31520-12 resin (PL) using a mechanical mixer for 2 hours at different speeds increasing from 100 rpm to 1500 rpm. For each test, 10 g of each resin batch with the curing agent in a (1:99) proportion were mixed vigorously for 2 minutes to ensure that a homogeneous mixture was achieved. The experiments were started immediately after the curing agent was mixed with the resin.

Table 4. The three resin mixtures with different graphene contents.

Sample ID	Graphene Content (wt%)	Description
Neat resin	0	Polylite 31520-12
PL+1 wt% GP	1	Polylite 31520-12 with 1 wt% graphene
PL+3 wt% GP	3	Polylite 31520-12 with 3 wt% graphene
PL+7 wt% GP	7	Polylite 31520-12 with 7 wt% graphene

3.3 Experimental Measurements

The cure kinetics of this resin system is studied using the TA Instruments Q100 Differential Scanning Calorimeter (DSC). 10 mg of each sample was used to perform dynamic tests at 5 °C/min from -30 °C to 250 °C. The Anton Paar MCR 302 rheometer was used for the rheological studies. The tests were performed using parallel plates (25 mm in diameter) from room temperature up to 70 °C at 5 °C/min. All the tests were repeated at least 3 times to ensure repeatability of the results.

4 Results and Discussion

4.1 Materials Characterization: Chemo-rheological Properties

According to the results of the DSC analysis, the addition of graphene does not have a significant effect on the curing profile of Polylite 31520-12 as shown in Figure 2(a). The initial study of the neat resin curing behaviour shows that this resin cures very rapidly at 55 °C. There are multiple additives and accelerators in this system which allows such rapid curing as the temperature reaches 55 °C. The heat flow curves do not show a significant decrease or increase in curing behaviour with the addition of graphene.

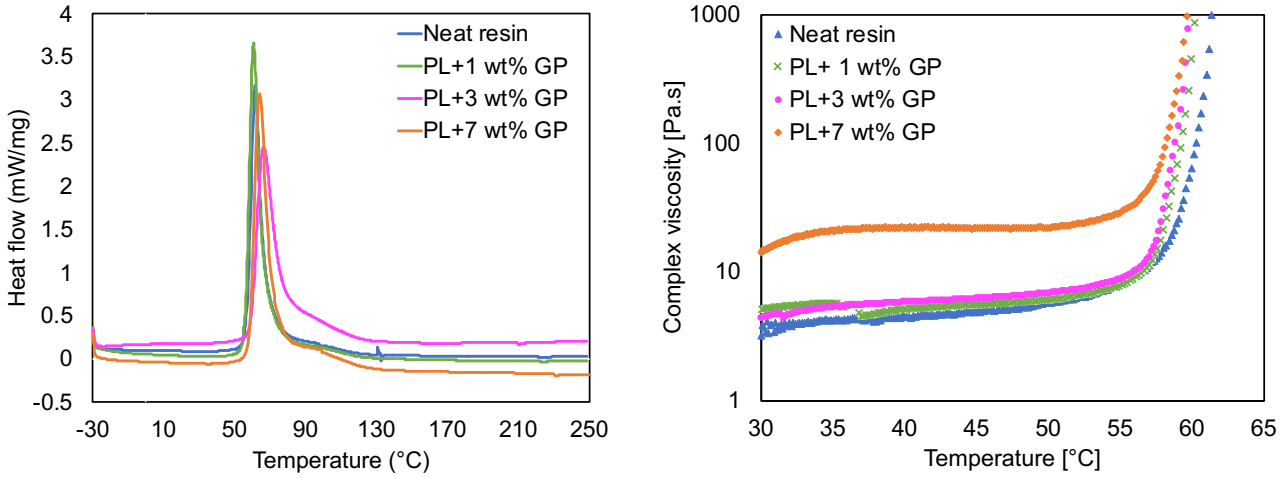

(a) (b)

Figure 2. Variation of (a) heat flow and (b) complex viscosity during the curing of the resin with different graphene content. The tests were done at 5 °C/min.

The results of the rheology tests are depicted in Figure 2 (b). Firstly, the linear viscoelastic region of the resin was determined by a running a frequency sweep test. Then, dynamic tests at 5 °C/min were performed from room temperature until 70 °C. The results show that by addition of graphene, the gel temperature decreases by two degrees which can be attributed to high thermal conductivity of the graphene in the nanocomposite [16]. The viscosity of the resin is another important factor that is impacted by the addition of graphene. It can be observed that the viscosity of the neat resin is 4.2 ± 0.18 Pa.s at 40 °C and it increases to 5.7 ± 0.57 Pa.s and 6.3 ± 0.26 Pa.s for the nanomodified resin with 1 wt% and 3 wt% graphene, respectively. For the nanomodified resin with 7 wt% graphene, the viscosity increases drastically to 21.9 ± 0.79 Pa.s.

4.2 Process Simulation: Analytical Results

Three C-RTM processing strategies were investigated: In-plane radial. In-plane rectilinear and transverse rectilinear. For the in-plane C-RTM strategy, it is assumed that the injection port is 0.2 m diameter (radial) or width (rectilinear). The injection pressure during the first phase is constant at 600 kPa and the compression rate in the second phase is -0.01 mm/s for a compression time of $t_{compression}$ equal to 100 seconds. For the transverse strategy, the injection is performed at atmospheric pressure and the compression phase is similar to the in-plane case. The permeability and stress functions of the preform studied here are adapted from the work of Bickerton and Abdullah [15] as described in Equations 1 and 2 respectively. This preform is a chopped glass fibre strand mat (CSM) with isotropic behaviour and its properties are summarized in Table 5.

$$K(V_f) = 5.42E-08.\exp(-18.6V_f), \quad 0.10 \le V_f \le 0.30, \tag{1}$$

$$\sigma(V_f) = 14500.\exp(12.0V_f) - 26420, \quad 0.10 \le V_f \le 0.30, \tag{2}$$

Table 5. Properties of the chopped strand mat preform.

Layer areal weight (g/cm^2)	200
Fibre density (g/cm^3)	2.6
Number of layers	9

The viscosity of the resin mixtures is assumed to be constant during injection and compaction and have a value of 4.2, 5.7, 6.3 and 21.9 Pa.s for the neat resin, PL+1 wt%, PL+3 wt% and PL+7 wt%, respectively.

4.2.1 In-plane Radial Strategy

For this case, the part has a radius of 0.56 m and a final thickness of 5 mm which gives a total volume of 0.005 m^3. Figure 1 (a) provides a schematic of the part studied. The mould cavity is assumed to be at 6 mm initially. The viscosity of the neat resin and nanomodified resins were input in the equations introduced in Table 1. Figure 3 (a) depicts the total clamp force evolution as the resin flows through the preform. It is observed that the total force is constant during the injection stage. The porosity of the preform does not change during this period and when the required amount of resin is injected, the flow front position is at 0.504 m. Then, the injection port closes, and the compaction stage starts. The preform is compressed until it reaches the final thickness and the resin fully saturates the preform. Thus, the total clamp force is due to the preform compression stress and fluid pressure. For the neat resin, the maximum force applied to the tooling is 136 kN at the end of compaction stage when the mould reaches final cavity thickness. This force increases to 167 kN, 179 kN and 506 kN for the PL+1 wt% GP, PL+3 wt% GP and PL+7 wt% GP mixtures, respectively.

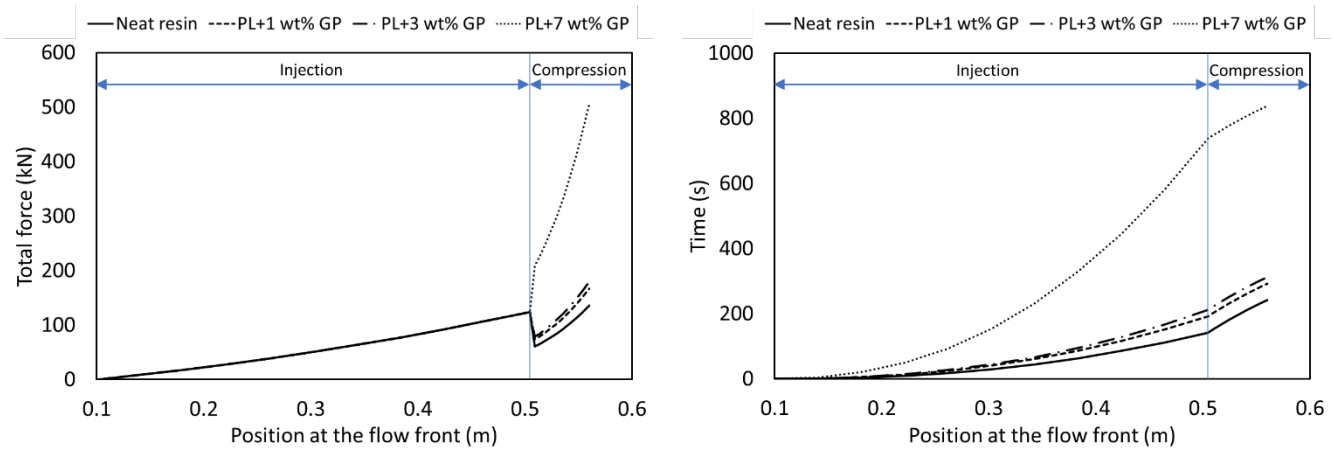

Figure 3. Effect of graphene content on (a) the total clamp force and (b) the filling time for the radial resin flow (Figure 1 (a)).

The filling time for the three resin formulations are compared in Figure 3 (b). This graph shows the relation between the resin flow front position and the time needed to reach that position. It can be seen that the injection stage lasts 141 s for the neat resin and it increases to 192 s, 212 s and 738 s for the systems with 1 wt%, 3 wt% and 7 wt% graphene, respectively. Considering that the compaction stage lasts 100 s for all resin systems, the total filling time

for the PL+7 wt% GP is more than 3.5 time of the neat resin. Thus, the filling time for the neat resin is less than 4 minutes while for the resin with 1 wt% and 3 wt% graphene it increases to almost 5 minutes and for the 7 wt% the filling time is 14 minutes. These results do not take into account the time needed to place the preforms in the mould and demould the cure part.

4.2.2 In-plane Rectilinear Strategy

For this case, the part is assumed to have a square shape with 1 m × 1 m dimensions and a final thickness of 5 mm. Thus, the total volume of this part is the same as the circular part equal to 0.005 m^3. The schematic of the part studied is depicted in Figure 1 (b). The initial mould cavity height is 6 mm. The injection port is placed in the centre of the part and has 1 m length and 0.2 m width. The viscosity of the neat resin and nanomodified resins were input in the equations introduced in Table 2. Figure 4 (a) depicts the total clamp force as the resin flows through the preform. Similar to the radial flow, the total force during injection is constant. The flow front position after the required amount of resin is injected is at 0.406 m. At this point the compaction stage starts and the total increase due to fluid pressure and preform compression stress. The total force at the end of the compaction is 1407 kN for the neat resin. It can be observed that this force reaches extremely high values for the nanomodified resin mixtures.

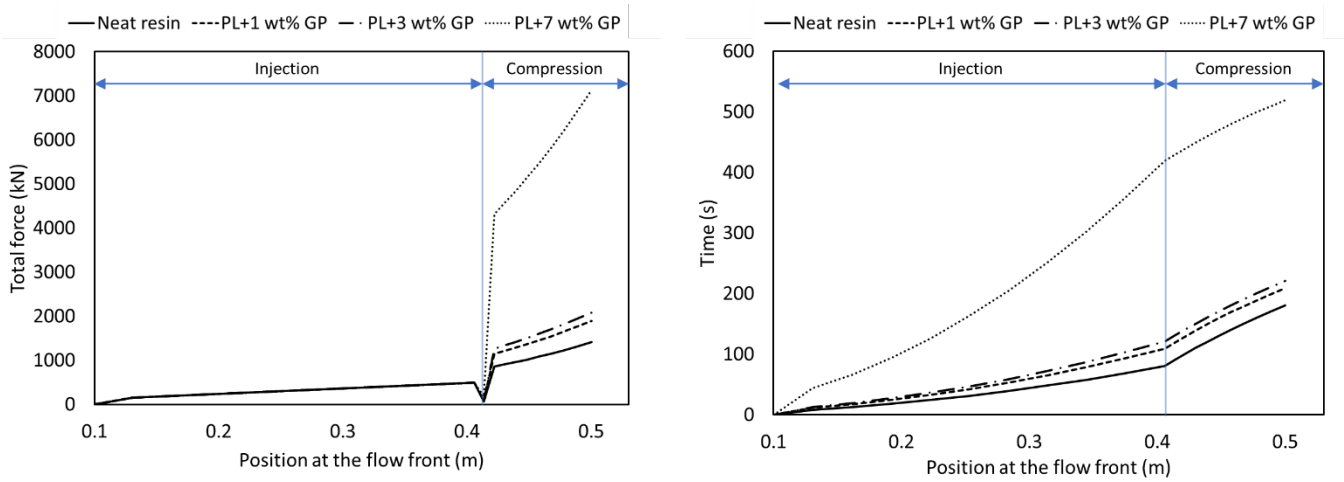

Figure 4. Effect of graphene content on (a) the total clamp force and (b) the filling time for the rectilinear resin flow (Figure 1 (b)).

The comparison of the filling time between different mixtures and viscosities is shown in Figure 4 (b). The injection time for the neat resin is 80 s and this number increases up to 109 s, 121 s and 519 s for the resin with 1 wt%, 3 wt% and 7 wt% graphene. Thus, the total filling time is 1.3 min for the neat resin, and it increases up to 1.8 min, 2 min, and 8.6 min for the PL+1 wt% GP, PL+3 wt% GP and PL+7 wt% GP.

4.2.3 Transverse Rectilinear Strategy

For this case, the part is assumed to have the same dimensions as the in-plane rectilinear preform. In such process, after placing the preforms in the lower mould cavity, the required volume of resin is first sprayed (manually or automatically) to cover the top area of the preform completely (resin-application stage). The preform has an initial thickness (h_i) of 6 mm. Then, the mould platen is lowered compressing the resin into the preform (compression stage). In this scenario, the resin flows transversely through the preform thickness as depicted in Figure 1 (c). For

the sake of comparison, it is assumed that the resin-application stage would take 100 s. Thus, the target volume of resin is injected at a constant rate Q_o. The compression rate is assumed to be 0.01 mm/s, thus, the compression stage would take 100 s, as well. Consequently, the total filling time is 200 s regardless of resin viscosity as shown in Figure 5 (a). The rest of the processing parameters such as resin viscosities, initial preform thickness, final part dimensions, compression rate, and preform properties were input in the equations introduced in Table 3.

During the injection stage, the resin infuses into the preform and its flow front position is 4.87 mm deep in the preform at the end of this stage. Then the mould closes at a constant rate until the preform is compressed to its final thickness and the section of dry preform is saturated with resin. Since the resin application is done in an open mould, there are no tooling forces in this stage. However, in the compression stage, there are two clamp forces due to resin infusion and preform compaction. Figure 5 (b) shows total clamp force during the compression stage in this transverse-CRTM process. The final force required in the compression stage is 50.073 ± 0.09 kN for the four resin systems in this study. The dominant force here is due to compaction of the preform from 6 mm to 5 mm. Since the resin travels a very short distance, the required force for resin infusion is very small and the resin viscosity does not have a significant impact on the total clamp force. Therefore, using a transverse-CRTM process, enables the adoption of higher graphene contents with shorter processing cycles and lower tooling forces.

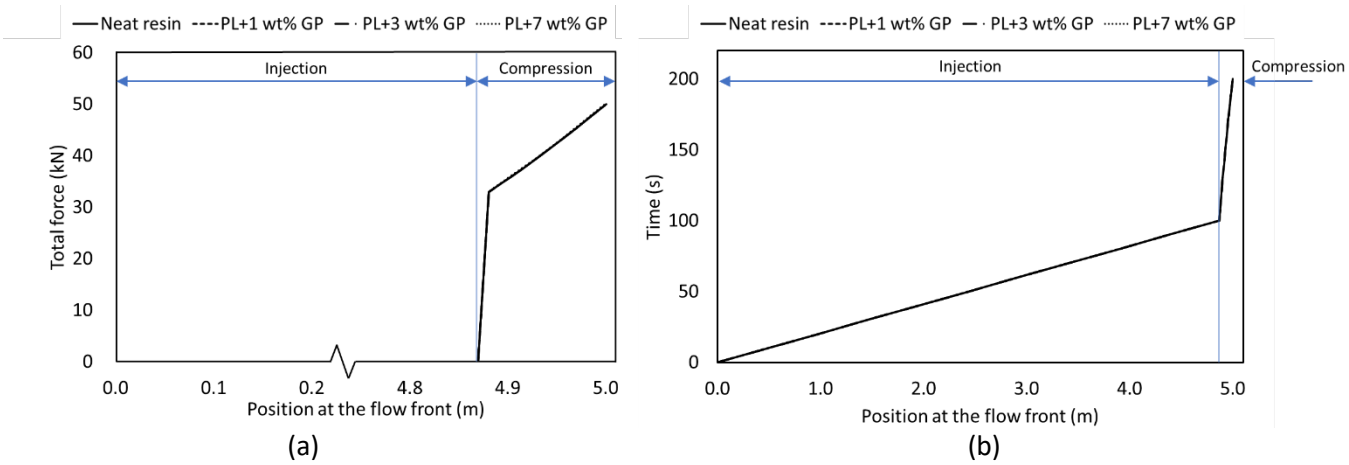

Figure 5. Effect of graphene content on the (a) total clamp force and (b) filling time for the transverse-CRTM process.

4.2.4 Discussion

One important conclusion which can be adapted from these calculations is determining if the resin mixture is still suitable for a given C-RTM processing strategy. One of the main advantages of C-RTM process is the short cycle time which can lead to producing up to 90000 part per year. The addition of graphene can introduce new properties (e.g. electrical conductivity) and improve existing properties (e.g. thermal conductivity and mechanical properties) [17–19], however, at high graphene contents, the viscosity of the nanomodified resin and thus, the filling time for each cycle can increase drastically. It is worth noting that the processability of systems with lower graphene contents (below 1 wt%) is less affected by the addition of graphene since the viscosity of the resin in those systems would still be less than the viscosity of nanomodified resin with 1 wt% graphene which is 5.7 Pa.s. Furthermore, the resin systems used in C-RTM processes are chemically engineered to gel under such short processing cycles and addition of graphene can increase the filling time and change the gel time and temperature. Gelation of the resin before completely filling the preform can lead to voids, dry spots in the preform and even clogging of the injection port. Thus, the filling time should be less than the resin gel time at the processing temperature. It is clear from this analysis

that the in-plane flow strategy is very sensitive to the resin viscosity and can lead to unacceptable cycle times and clamping forces. However, a transverse impregnation strategy is very robust and more compatible for the processing of nanomodified resins. Furthermore, as the flow distance is reduced, nanoparticles filtration effects will also be minimized [17, 18].

5 Conclusion

In this study, the effect of a mass-produced graphene on the thermo-rheological properties of an RTM-grade unsaturated polyester resin was studied. The results show that the gel temperature and viscosity of the nanomodified resin is affected by the graphene content. Analytical solutions showed the effect of the variation in resin viscosity on the filling time and clamp force in a C-RTM process for different injection-compression strategies. This study illustrates the importance of selecting the proper injection strategy in order to process nanomodified resin systems. Finally, resins with low graphene content (less than 1% wt% GP) behave like the neat resin system and can be processed in similar conditions.

6 Acknowledgements

The authors would like to thank the funding partners PRIMA Quebec, The Natural Sciences and Engineering Research Council of Canada (NSERC) and Nanoxplore Inc. The authors also thank Emi Myzeqari for her help with the characterization tests.

7 References

[1] D. Matykiewicz, “Hybrid epoxy composites with both powder and fiber filler: A review of mechanical and thermomechanical properties,” *Materials (Basel).*, vol. 13, no. 8, 2020.

[2] K. S. Novoselov, “Electric Field Effect in Atomically Thin Carbon Films,” *Science (80-.).*, vol. 306, no. 5696, pp. 666–669, Oct. 2004.

[3] M. Rafiee, S. H. Rad, F. Nitzsche, J. Laliberte, and M. R. Labrosse, “Significant fatigue life enhancement in multiscale doubly-modified fiber/epoxy nanocomposites with graphene nanoplatelets and reduced-graphene oxide,” *Polymers (Basel).*, vol. 12, no. 9, 2020.

[4] M. Lakshmanan, K. Jayanarayanan, and J. Joesph, “An Experimental Investigation of Fracture Toughness and Volume Resistivity of Symmetric Laminated Epoxy/Glass Fiber/CNT multiscale composites,” *IOP Conf. Ser. Mater. Sci. Eng.*, vol. 577, no. 1, 2019.

[5] J. Zhang *et al.*, “Effect of hierarchical structure on electrical properties and percolation behavior of multiscale composites modified by carbon nanotube coating,” *Compos. Sci. Technol.*, vol. 164, no. May, pp. 160–167, Aug. 2018.

[6] N. L. Batista *et al.*, “Mass-produced graphene—HDPE nanocomposites: Thermal, rheological, electrical, and mechanical properties,” *Polym. Eng. Sci.*, vol. 59, no. 4, pp. 675–682, Apr. 2019.

[7] L. R. Melo de Lima *et al.*, “Characterization of commercial graphene-based materials for application in thermoplastic nanocomposites,” *Mater. Today Proc.*, vol. 20, pp. 383–390, 2018.

[8] J. Barroeta Robles *et al.*, “Processing and properties of graphene-enhanced glass fibre composites using a scalable manufacturing process,” *Compos. Struct.*, vol. 267, no. October 2020, 2021.

[9] K. Yang *et al.*, “The thermo-mechanical response of PP nanocomposites at high graphene loading,” *Nanocomposites*, vol. 1, no. 3, pp. 126–137, 2015.

[10] F. Kargar *et al.*, “Thermal Percolation Threshold and Thermal Properties of Composites with High Loading of Graphene and Boron Nitride Fillers,” *ACS Appl. Mater. Interfaces*, vol. 10, no. 43, pp. 37555–37565, 2018.

[11] A. Vita, V. Castorani, M. Germani, and M. Marconi, “Comparative life cycle assessment of low-pressure RTM, compression RTM and high-pressure RTM manufacturing processes to produce CFRP car hoods,” *Procedia CIRP*, vol. 80, pp. 352–357, 2019.

[12] Z. Sun *et al.*, “Preparation of high-performance carbon fiber-reinforced epoxy composites by compression resin transfer molding,” *Materials (Basel).*, vol. 12, no. 1, 2018.

[13] F. A. Martin *et al.*, “Simulation and Validation of Injection-Compression Filling Stage of Liquid Moulding with Fast Curing Resins,” *Appl. Compos. Mater.*, vol. 26, no. 1, pp. 41–63, 2019.

[14] P. Hubert, C. Demaria, C. Keulen, C. Mobuchon, and A. Poursartip, “Development of a workflow for the design of liquid composite moulding processes,” 2014.

[15] S. Bickerton and M. Z. Abdullah, “Modeling and evaluation of the filling stage of injection/compression moulding,” *Compos. Sci. Technol.*, vol. 63, no. 10, pp. 1359–1375, 2003.

[16] M. G. Prolongo, C. Salom, C. Arribas, M. Sánchez-Cabezudo, R. M. Masegosa, and S. G. Prolongo, “Influence of graphene nanoplatelets on curing and mechanical properties of graphene/epoxy nanocomposites,” *J. Therm. Anal. Calorim.*, vol. 125, no. 2, pp. 629–636, 2016.

[17] R. Moriche, M. Sánchez, A. Jiménez-Suárez, S. G. Prolongo, and A. Ureña, “Electrically conductive functionalized-GNP/epoxy based composites: From nanocomposite to multiscale glass fibre composite material,” *Compos. Part B Eng.*, vol. 98, pp. 49–55, 2016.

[18] L. Liu, H. Wang, M. Shan, Y. Jiang, X. Zhang, and Z. Xu, “Lightweight sandwich fiber-welded foam-like nonwoven fabrics/graphene composites for electromagnetic shielding,” *Mater. Chem. Phys.*, vol. 232, no. February, pp. 246–253, 2019.

[19] M. Rafiee, F. Nitzsche, J. Laliberte, S. Hind, F. Robitaille, and M. R. Labrosse, “Thermal properties of doubly reinforced fiberglass/epoxy composites with graphene nanoplatelets, graphene oxide and reduced-graphene oxide,” *Compos. Part B Eng.*, vol. 164, no. November 2018, pp. 1–9, May 2019.

[20] H. Zhang *et al.*, “Filtration effects of graphene nanoplatelets in resin infusion processes: Problems and possible solutions,” *Compos. Sci. Technol.*, vol. 139, pp. 138–145, 2017.

[21] M. Yourdkhani, W. Liu, S. Baril-Gosselin, F. Robitaille, and P. Hubert, “Carbon nanotube-reinforced carbon fibre-epoxy composites manufactured by resin film infusion,” *Compos. Sci. Technol.*, vol. 166, pp. 169–175, 2018.